



# Symmetrical and Unsymmetrical Fault Currents of a Wind Power Plant

## Preprint

V. Gevorgian, M. Singh, and E. Muljadi

*To be presented at the IEEE Power and Energy Society General Meeting  
San Diego, California  
July 22-26, 2012*

NREL is a national laboratory of the U.S. Department of Energy, Office of Energy Efficiency & Renewable Energy, operated by the Alliance for Sustainable Energy, LLC.

**Conference Paper**  
NREL/CP-5500-53463  
December 2011

Contract No. DE-AC36-08GO28308

## NOTICE

The submitted manuscript has been offered by an employee of the Alliance for Sustainable Energy, LLC (Alliance), a contractor of the US Government under Contract No. DE-AC36-08GO28308. Accordingly, the US Government and Alliance retain a nonexclusive royalty-free license to publish or reproduce the published form of this contribution, or allow others to do so, for US Government purposes.

This report was prepared as an account of work sponsored by an agency of the United States government. Neither the United States government nor any agency thereof, nor any of their employees, makes any warranty, express or implied, or assumes any legal liability or responsibility for the accuracy, completeness, or usefulness of any information, apparatus, product, or process disclosed, or represents that its use would not infringe privately owned rights. Reference herein to any specific commercial product, process, or service by trade name, trademark, manufacturer, or otherwise does not necessarily constitute or imply its endorsement, recommendation, or favoring by the United States government or any agency thereof. The views and opinions of authors expressed herein do not necessarily state or reflect those of the United States government or any agency thereof.

Available electronically at <http://www.osti.gov/bridge>

Available for a processing fee to U.S. Department of Energy and its contractors, in paper, from:

U.S. Department of Energy  
Office of Scientific and Technical Information

P.O. Box 62  
Oak Ridge, TN 37831-0062  
phone: 865.576.8401  
fax: 865.576.5728  
email: <mailto:reports@adonis.osti.gov>

Available for sale to the public, in paper, from:

U.S. Department of Commerce  
National Technical Information Service  
5285 Port Royal Road  
Springfield, VA 22161  
phone: 800.553.6847  
fax: 703.605.6900  
email: [orders@ntis.fedworld.gov](mailto:orders@ntis.fedworld.gov)  
online ordering: <http://www.ntis.gov/help/ordermethods.aspx>

Cover Photos: (left to right) PIX 16416, PIX 17423, PIX 16560, PIX 17613, PIX 17436, PIX 17721



Printed on paper containing at least 50% wastepaper, including 10% post consumer waste.

# Symmetrical and Unsymmetrical Fault Currents of a Wind Power Plant

V. Gevorgian

Member IEEE  
vahan.gevorgian@nrel.gov

M. Singh

Member IEEE  
mohit.singh@nrel.gov

E. Muljadi

Fellow, IEEE  
eduard.muljadi@nrel.gov

National Renewable Energy Laboratory  
1617 Cole Blvd.  
Golden, CO 80401, USA

**Abstract** – The size of wind power plants (WPPs) keeps getting bigger and bigger. The number of wind plants in the U.S. has increased very rapidly in the past 10 years. It is projected that in the U.S., the total wind power generation will reach 330 GW by 2030. As the importance of WPPs increases, planning engineers must perform impact studies used to evaluate short-circuit current (SCC) contribution of the plant into the transmission network under different fault conditions. This information is needed to size the circuit breakers, to establish the proper system protection, and to choose the transient suppressor in the circuits within the WPP. This task can be challenging to protection engineers due to the topology differences between different types of wind turbine generators (WTGs) and the conventional generating units.

This paper investigates the short-circuit behavior of a WPP for different types of wind turbines. Both symmetrical faults and unsymmetrical faults are investigated. Three different software packages are utilized to develop this paper. Time domain simulations and steady-state calculations are used to perform the analysis.

**Index Terms** — Fault contribution, induction generator, protection, short circuit, wind power plant, and wind turbine.

## I. INTRODUCTION

Energy and environmental issues have become one of the biggest challenges facing the world. In response to energy needs and environmental concerns, renewable energy technologies are considered the future technologies of choice [1], [2]. Renewable energy is harvested from nature, and it is clean and free. However, it is widely accepted that renewable energy is not a panacea that comes without challenges. With the federal government's aggressive goal of achieving 20% wind energy penetration by 2030, it is necessary to understand the challenges that must be overcome when using renewable energy.

In the years to come, there will be more and more wind power plants (WPPs) connected to the grid. With the goal of 20% wind penetration by 2030, the WPP's operation should be well planned. The power system switchgear and power system protection for WPPs should be carefully designed to be compatible with the operation of conventional synchronous generators connected to the same grid. This paper attempts to illustrate the behavior of short-circuit current (SCC) contributions for different types of WTGs.

The power system model used for WPP short-circuit behavior simulation was adopted from a modeling guide devel-

oped by the Western Electricity Coordinating Council (WECC) Wind Generator Modeling and Validation Work Group (WGMG) [3]. The WGMG recommends the use of a single-machine equivalent representation of multiple wind turbines operating in a single WPP. Based on industry experience, this representation is also considered adequate for positive-sequence transient-stability simulations. The WECC single-machine equivalent representation of a WPP is shown in Figure 1. The interconnection transmission lines, transformers, and reactive power compensation are present in this representation.

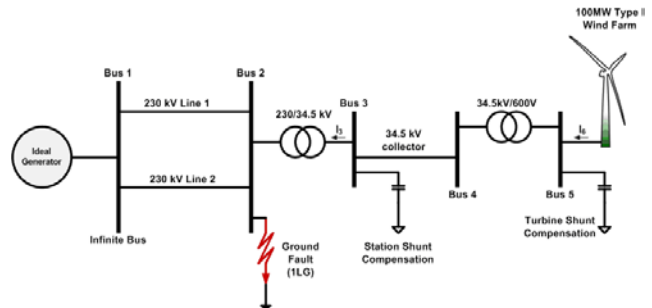


Figure 1: A single-machine equivalent representation of a WPP

## Organization of the Paper

The organization of this paper is as follows; in section II, the SCC characteristics of different WTG types will be presented for a symmetrical fault. In section III, the characteristics of SCC for unsymmetrical faults will be discussed. Finally, in section V, the conclusion will summarize the paper's findings. Detailed dynamic modeling of four different types of WTGs is simulated in PSCAD<sup>TM</sup>.

## II. SHORT-CIRCUIT BEHAVIOR UNDER SYMMETRICAL FAULTS

A utility-sized wind turbine is larger than non-grid wind turbine applications. In the early days, the turbines were sized from 10 kW to 100 kW. Nowadays, wind turbines are sized above 1000 kW (1 MW).

### A. SCC from a Type 1 WTG

The first generation of utility-sized WTGs were fixed-speed turbines with a squirrel-cage induction generator (SCIG) and is called a Type I generator in wind-related applications. The SCIG generates electricity when it is driven above synchronous speed. Normal operating slips for an in-

duction generator are between 0% and -1%. The simplified single-phase equivalent circuit of a squirrel-cage induction machine is shown in Figure 2 [4].

The circuit in Figure 2 is referred to the stator side where  $R_s$  and  $R_r$  are stator and rotor resistances,  $L_{s\sigma}$  and  $L_{r\sigma}$  are stator and rotor leakage inductances,  $L_m$  is magnetizing reactance, and  $s$  is rotor slip. The example single-line connection diagram of a Type I generator is shown in Figure 3. In the case of a fault, the inertia of the wind rotor drives the generator after the voltage drops at the generator terminals, the pitch controller must be deployed to avoid a run-away problem. The rotor flux may not change instantaneously right after the voltage drop due to a fault. Therefore, voltage is produced at the generator terminals causing fault current flow into the fault until the rotor flux decays to zero. This process takes a few electrical cycles. The fault current produced by an induction generator must be considered when selecting the rating for circuit breakers and fuses. The fault current is limited by generator impedance (and can be calculated from parameters in Figure 2) and impedance of the system from the short circuit to the generator terminals.

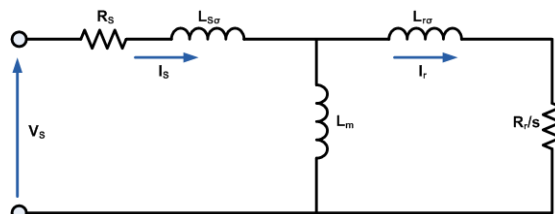


Figure 2: Equivalent circuit of a Type 1 generator

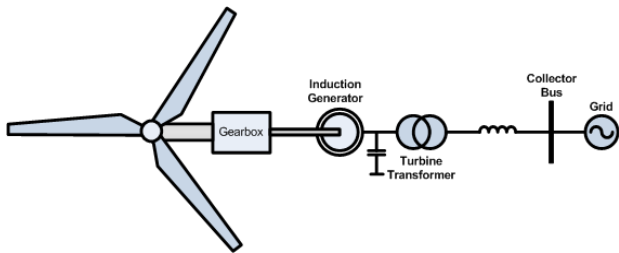


Figure 3: Connection diagram for a Type 1 WTG

The initial value of fault current fed in by the induction generator is close to the locked rotor-inrush current. Assuming a three-phase symmetrical fault, an analytical solution can be found to estimate the current contribution of the generator. The SCC of an induction generator can be calculated as [5]:

$$i(t) = \frac{\sqrt{2}V_s}{Z'_s} \left[ e^{-\frac{t}{T'_s}} \sin(\alpha) - (1 - \sigma)e^{-\frac{t}{T'_r}} \sin(\omega t + \alpha) \right] \quad (1)$$

Where  $\alpha$  is the voltage phase angle for a given phase,  $\sigma$  is the leakage factor,  $Z'_s = X'_s = \omega L'_s$  is stator transient reactance, and  $T'_s$  and  $T'_r$  are stator and rotor time constants representing the damping of the DC component in stator and rotor windings. The transient stator and rotor inductances  $L'_s$  and  $L'_r$  can be determined from the equation (2).

$$L'_s = L_{s\sigma} + \frac{L_r \sigma L_m}{L_r \sigma + L_m} \quad L'_r = L_{r\sigma} + \frac{L_s \sigma L_m}{L_s \sigma + L_m} \quad (2)$$

$$T'_s = \frac{L'_s}{R_s} \quad T'_r = \frac{L'_r}{R_r} \quad (3)$$

$$\sigma = 1 - \frac{L_m^2}{L_s L_r} \quad (4)$$

$$L_s = L_{s\sigma} + L_m \quad L_r = L_{r\sigma} + L_m \quad (5)$$

As shown in Figure 4, the fault current is driven by the decaying flux trapped in the rotor winding as represented by the right portion of equation (1). The larger the leakage inductances ( $\sigma$ ), the smaller is the fault current amplitude. The fault current dies out after the flux driving the fault current depleted to zero. Note that the DC and AC transient components of the SCC flowing out of the stator windings induce fault currents in the rotor winding and vice versa until the magnetic flux is depleted.

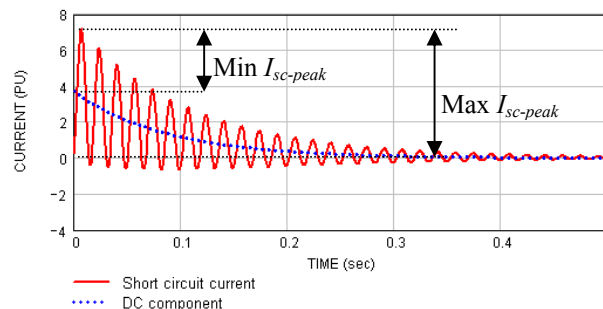


Figure 4: SCC from a Type 1 WTG

The current calculated from equation (4) is shown in Figure 4 using parameters for a typical 2-MW induction generator when and pre-fault voltage of 0.7 p.u. The current reaches the maximum value at  $\pi$  (first half a period). Therefore, it may be a good approximation to calculate the maximum (peak) current by substituting  $t = T/2$  into (1). The resulting equation for peak current will be:

$$i_{max} = \frac{\sqrt{2}V_s}{Z'_s} \left[ e^{-\frac{T}{2T'_s}} + (1 - \sigma)e^{-\frac{T}{2T'_r}} \right] \quad (6)$$

It was demonstrated experimentally in [6] that equation (6) gives satisfactory accuracy for peak current assessment.

### C. SCC from a Type 2 WTG

The variable slip generator is essentially a wound-rotor induction generator with a variable resistor connected in series to the rotor winding (for Type 2 WTGs, refer to Figure 5 and Figure 6).

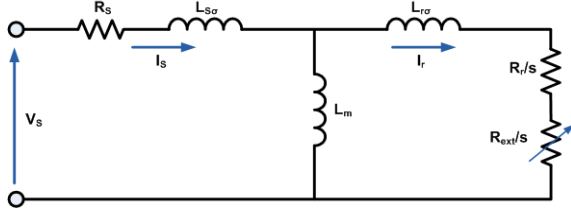


Figure 5: Equivalent circuit for a Type 2 generator

The modified rotor time constant can be calculated by adding the effect of the external resistor  $R_{ext}$ , where  $R_{ext}$  is the value of external resistance that happens to be in the circuit at the time of the fault. So, adding the external resistors increases the overall rotor resistance.

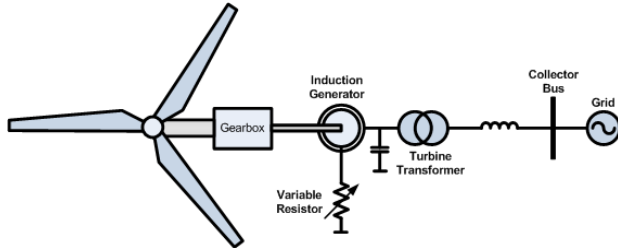


Figure 6: Connection diagram for a Type 2 WTG

#### D. SCC from a Type 3 WTG

A Type 3 WTG is implemented by a doubly-fed induction generator (DFIG). It is a variable speed WTG where the rotor speed is allowed to vary within a slip range of  $\pm 30\%$ . Thus, the power converter can be sized to about 30% of rated power. The DFIG equivalent circuit is similar to one for a regular induction generator except for additional rotor voltage, representing voltage produced by a power converter. Under normal operation, this voltage is actually from a current-controlled power converter with the ability to control the real and reactive power output instantaneously and independently.

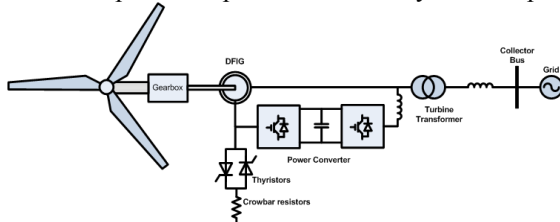


Figure 7: Connection diagram for a Type 3 WTG

The typical connection diagram for a DFIG (Type 3) WTG is shown in Figure 7. In an ideal situation, the power converter connected to the rotor winding should be able to withstand the currents induced by the DC and AC components flowing in the stator winding. However, the components of the power converter (IGBT, diode, and capacitor, etc) are designed to handle only normal currents and normal DC bus voltage. A crowbar system is usually used for protecting the power electronics converter from overvoltage and thermal breakdown during short-circuit faults. A crowbar is usually implemented to allow the insertion of additional resistance into the rotor winding to divert the SCC in the rotor winding

from damaging the power converter. Additional dynamic braking on the DC bus is also used to limit the DC bus voltage.

#### E. Type 4 WTGs

A typical connection diagram for a Type 4 WTG is shown in Figure 8. The SCC contribution for a three-phase fault is limited to its rated current or a little above its rated current. It is common to design a power converter for a Type 4 wind turbine with an overload capability of 10% above rated. Note that in any fault condition, the generator stays connected to the power converter and is buffered from the faulted lines on the grid.

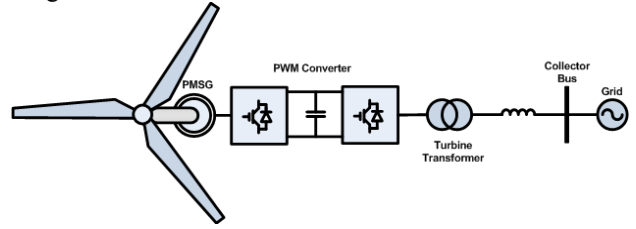


Figure 8: PMSG direct-drive WTG diagram

#### F. SCC Comparison for Symmetrical Faults

The SCC for different types of wind turbines are not the same. For each turbine type, the peak value of the magnitude of the SCC is affected by the transient reactance, the pre-fault voltage, the effective rotor resistances, and other circumstances at the instant the fault occurs.

As shown in Figure 9, the Type 1 WTG has the largest SCC and the shortest settling time. The Type 2 WTG has an additional rotor resistance that is activated above rated wind speed to limit the output power of the generator. Below rated wind speed, the SCC behavior of the Type 2 WTG is similar to the Type 1 WTG. Above rated wind speed, the SCC behavior of Type 2 WTG is affected by the external rotor resistance. The settling time of the SCC of Type 2 WTG is lower than the settling time of the SCC of Type 1 WTG.

The SCC behavior of the Type 3 WTG is affected by the crowbar and the dynamic braking actions. For a very near fault, the crowbar may be fully deployed and thus, short-circuiting the rotor winding, and the SCC behavior resembles the Type 1 WTG; however, if the crowbar and the dynamic braking can maintain the operation of the rotor side power converter, the SCC behavior is very close to a Type 4 WTG. For almost all of the SCC for Type 3 WTGs, only a small amount of SCC current is passed through the power converter because of the current limit of the power semiconductors.

The Type 4 WTG has a full power converter between the generator and the grid, thus, the SCC is very well regulated with SCC maintained at 1.1 p.u. rated current.

#### G. Summary of the Symmetrical Fault SCC

To summarize, the SCC for a symmetrical faults can be approximated by the values listed in Table I [7]. Both the maximum and the minimum values are shown.

TABLE I  
MAXIMUM AND MINIMUM POSSIBLE VALUE OF THE SCC

WTG	Type 1	Type 2	Type 3	Type 4
<b>Max</b> $I_{SC\_PEAK}$	$2 \frac{\sqrt{2}V_s}{X'_s}$	$2 \frac{\sqrt{2}V_s}{X'_s}$	$2 \frac{\sqrt{2}V_s}{X'_s}$	1.1 $I_{RATED}$
<b>Min</b> $I_{SC\_PEAK}$	$\frac{\sqrt{2}V_s}{X'_s}$	$\frac{\sqrt{2}V_s}{\sqrt{X_s'^2 + (9R_r')^2}}$	1.1 $I_{RATED}$	0

For a Type 1 WTG, the maximum SCC is based on the assumption that the DC offset is at the worst condition, and the minimum SCC is calculated by assuming that the DC offset is zero. For a Type 2 WTG, the maximum value is computed when  $R_{ext} = 0 \Omega$ . The minimum value is computed when the slip reaches 10% above synchronous speed. And for a Type 3 WTG, the maximum value is computed when the crowbar shorts the rotor winding and the minimum value is computed when the power converter can follow the commanded current (i.e., in case the fault occurs far away from the point of interconnection (POI), the remaining terminal voltage is sufficiently high enough to let the power converter operate normally and supply the commanded currents). Note that for a symmetrical fault, the actual fault current for each phase is different from the other phases due to the fact that the time of the fault occurs at a different phase angle for different phases, thus affecting the DC offset. For a Type 4 WTG, the stator current can always be controlled because of the nature of power converter, which is based on a current-controlled voltage source converter.

A time domain simulation is performed in PSCAD, and the steady-state calculations are performed using Mathcad and Cyme software for a symmetrical fault. The results are tabulated in Table II. The calculated results from different software platforms are very close to the approximation listed in Table I. Note, that only Type 1 and Type 4 are listed. The Type 2 and Type 3 WTGs will respond differently because of the existence of the external rotor resistance in a Type 2 WTG and the activation of the crowbar circuit in a Type 3 WTG, which will respond non-linearly to the fault. The SCC for a Type 2 and Type 3 WTG, as indicated in Table I, will have the size difference between the SCC of the Type 1 and Type 4 WTGs.

TABLE II  
 $I_{SC\_PEAK}$  COMPARISON FOR DIFFERENT SOFTWARE PLATFORMS

WTG Type	Table I		PSCAD	Cyme	Math- cad
	Min	Max			
1	3.4 p.u.	6.3 p.u.	5 p.u.	5.5 p.u.	3.8 p.u.
4	0 p.u.	1.1 p.u.	1.1 p.u.	1.1 p.u.	1.1 p.u.

### III. UNSYMMETRICAL FAULTS

The nature of the fault produces a different response for different wind turbine types. In this section, the observation of the short-circuit behavior for unsymmetrical faults on different types of WTGs will be presented.

Note that operating an induction generator under an unbalanced condition creates torque pulsation and unbalanced currents. If this condition persists for a long period of time, it may excite other parts of the wind turbine, and the unbalanced currents may create unequal heating in the three-phase windings, thus, shorten the life of the winding insulation.

Unlike in a symmetrical three-phase fault, the positive-sequence voltage source continues to drive the fault current during the fault. As shown in Figure 11 and Figure 12, the remaining un-faulted (normal) phases continue to maintain the air-gap flux. The initial conditions of the fault currents are different for each phase. The three line currents usually show a different DC offset, which eventually settles out over time.

#### A. Single Line-to-Ground (SLG) Faults

The single line-to-ground fault is the most likely to occur in

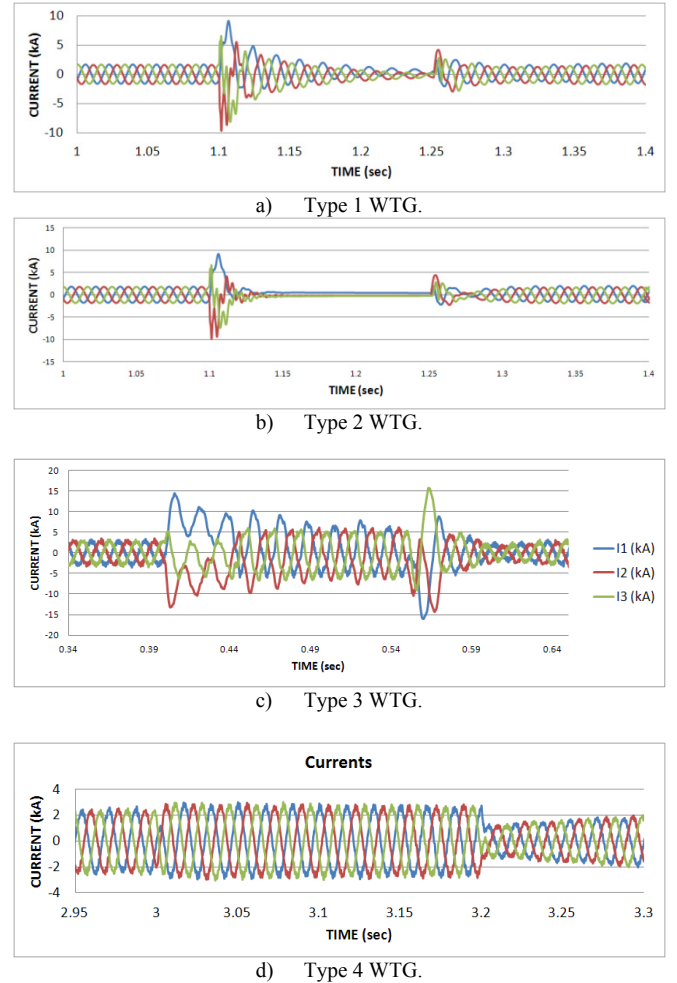


Figure 9: SCC of a symmetrical fault for four types of WTGs

a power system. The magnetic flux in the air gap, although smaller than normal and unbalanced, is maintained by the remaining un-faulted lines. Thus, the short circuit in SLG faults will continue to flow until the circuit breaker removes the fault from the circuit.

Figure 10 shows the sequence circuits of the WPP shown in Figure 1. The sequence circuits are arranged to compute the SLG fault currents. Although present in the actual simulation, the cable capacitance and the capacitor compensation shown in Figure 1 are not drawn in Figure 12 to avoid clutter and to simplify the drawing. We represent the transformer winding connections in the zero sequence equivalent circuit as an on-off switch indicating the availability of the zero sequence current path. Since the low side of the pad-mounted transformer is connected in delta, there is no sequence current flowing out of the WTG.

We also placed a switch at the negative sequence equivalent circuit for the WTG to indicate that there is no negative sequence current contribution from a Type 4 WTG because it is controlled to provide symmetrical currents regardless of the terminal voltage.

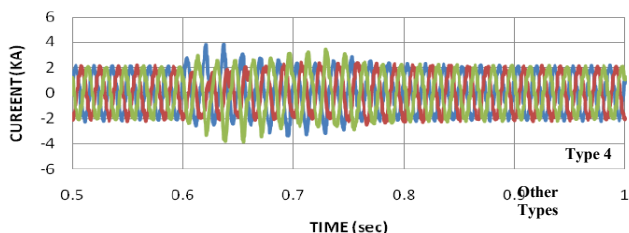


Figure 11: SCC for SLG for a Type 3 WTG

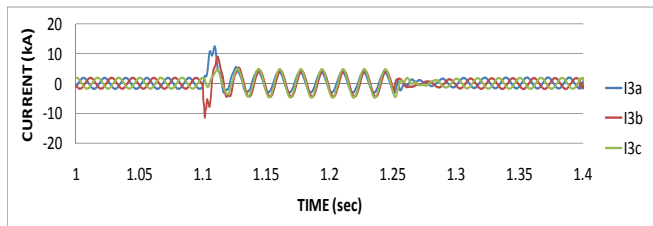


Figure 12: SCC for LLG fault of a Type 2 WTG

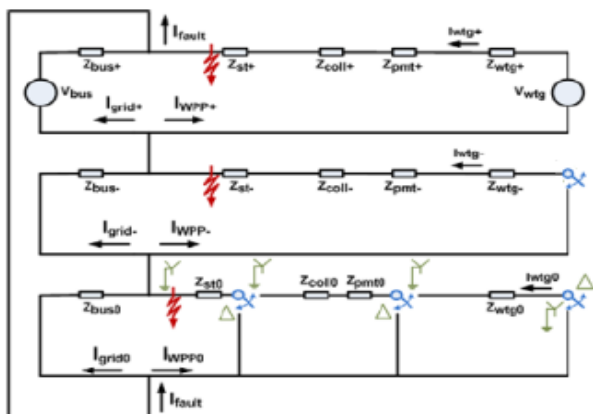


Figure 10: The equivalent circuit for an SLG fault

In Figure 13, the SCC for a Type 1 WTG is shown both for the three-phase currents and the corresponding sequence components. The changes in positive sequence and the sudden appearance of the negative sequence are also shown. The absence of the zero sequence current is a consequence of winding connections.

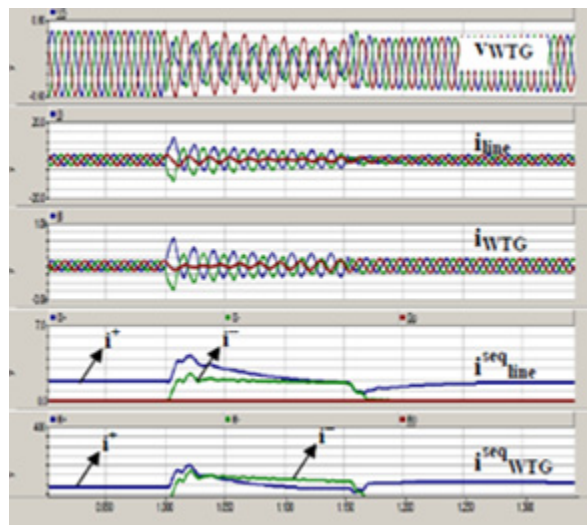


Figure 13: SCC for a single line-to-ground in a Type 1 WPP

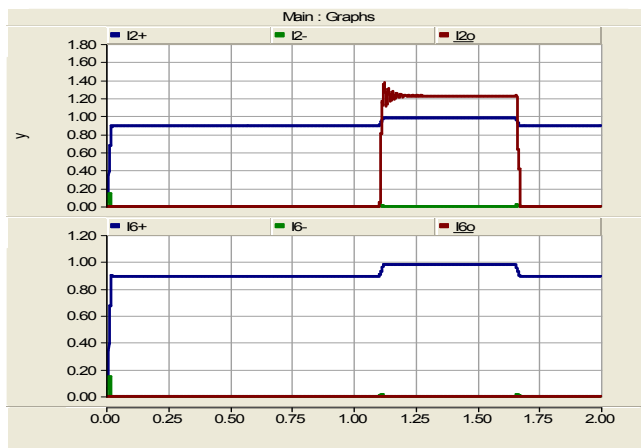


Figure 14: SCC for a single line-to-ground in a Type 4 WPP

- a) At the point of interconnection
- b) At the wind generator terminals

In Figure 14, the SCC for a Type 4 WTG shows the fault currents in its sequence current components. At the POI (Figure 14a), there exist both the zero sequence and the negative sequence currents because of the substation transformer winding connection ( $Y_g Y_g$ ) and collector system capacitances respectively. As shown in Figure 14b, at the generator terminals however, there is a pad-mounted transformer ( $Y_g \Delta$ ) that will block the zero sequence component, and the Type 4 WTG produces a positive sequence component (refer to negative sequence switch in the equivalent circuit shown Figure 12).

In Table III, the SCC at the POI is computed for a SLG fault using different software platform. It is shown that the

SCC results match for all software for Type 1 WTG. A small mismatch between the MathCAD and PSCAD results can be seen in Table 3. This discrepancy exists because in MathCAD, we remove the capacitances from the circuit.

TABLE III  
COMPUTED SCC AT THE POINT OF INTERCONNECTION OF THE WPP  
IN SEQUENCE COMPONENTS IN PER UNIT  
FOR AN SLG FAULT WITH DIFFERENT SOFTWARE PLATFORMS

WTG	I <sub>Seq</sub>	PSCAD	Cyme	Math-cad
Type 1	0	1.42	1.58	1.67
	1	0.58	0.57	0.55
	2	0.63	0.57	0.65
Type 4	0	1.4	1.44	1.35
	1	1.0	0.95	1.0
	2	0.25	0.0	0.0

TABLE IV  
COMPUTED SCC AT THE GENERATOR TERMINALS  
IN SEQUENCE COMPONENTS IN PER UNIT  
FOR AN SLG FAULT WITH DIFFERENT SOFTWARE PLATFORMS

WTG	I <sub>Seq</sub>	PSCAD	Cyme	MathCAD
Type 1	0	0.0	0.0	0.0
	1	0.58	0.56	0.55
	2	0.62	0.59	0.65
Type 4	0	0.0	0.0	0.0
	1	1.0	1.0	1.0
	2	0.0	0.0	0.0

In Table IV, the SCC at the generator terminal is computed for an SLG fault for Type 4 WTG. It is shown that the SCC results match for all software for a Type 4 WTG. Because of the mismatch between the MathCAD and the PSCAD results, we remove the capacitances in the circuit.



Figure 15: An example of typical output panel for SCC calculation with Cyme.

Comparing Table IV to Table III for a Type 4 turbine, it is shown that the zero sequence and negative sequence components do not exist. As shown in Figure 14, the absence of

zero and negative sequence currents can be observed at the generator terminals.

A snapshot of the computer output from Cyme is presented in Figure 15, where the line currents and the sequence currents are presented on the same output panel.

B. Line-to-Line (LL) and Line-to-Line-to-Ground (LLG) Faults

The line-to-line fault and the line-to-line-to-ground fault also maintained the air-gap flux during the fault. The SCC will continue to flow until the circuit breaker removes the fault from the circuit.

In Table V the SCC at the POI is presented for a LL fault. It is shown that we have a very good match between PSCAD, Cyme, and MathCAD calculations. The absence of the zero sequence current can be expected because the fault does not involve the ground.

TABLE V  
COMPUTED SCC AT THE POINT OF INTERCONNECTION OF THE WPP  
IN SEQUENCE COMPONENTS IN PER UNIT  
FOR AN LL FAULT WITH DIFFERENT SOFTWARE PLATFORMS

WTG	I <sub>Seq</sub>	PSCAD	Cyme	Mathcad
Type 1	0	0.0	0.0	0.0
	1	0.95	0.86	0.95
	2	0.8	0.86	1.05
Type 4	0	0.0	0.0	0.0
	1	1.0	1.0	1.0
	2	0.4	0.0	0.0

In Table VI, the SCC at the POI is presented for LLG fault. It is shown that we have a very good match between PSCAD, Cyme, and MathCAD calculations. In comparison to Table V, we can see the presence of the zero sequence current in LLG fault as expected in Table VI.

TABLE VI  
COMPUTED SCC AT THE POINT OF INTERCONNECTION OF THE WPP  
IN SEQUENCE COMPONENTS IN PER UNIT  
FOR AN LLG FAULT WITH DIFFERENT SOFTWARE PLATFORMS

WTG	I <sub>Seq</sub>	PSCAD	Cyme	Mathcad
Type 1	0	1.55	1.63	1.48
	1	1.17	1.11	1.1
	2	0.55	0.62	0.8
Type 4	0	1.4	1.49	1.7
	1	1	0.9	1
	2	0.25	0.0	0

As an illustration, the currents at the POI for LL faults and LLG faults for Type 1 WTGs are presented in Figure 16, and

the corresponding sequence components are presented in Figure 17. As shown in Figure 16, it is difficult to discern the type of faults that occur in the line. In comparison, from Figure 17, it is obvious there is a distinction between the fault currents for the LL fault and the LLG fault.

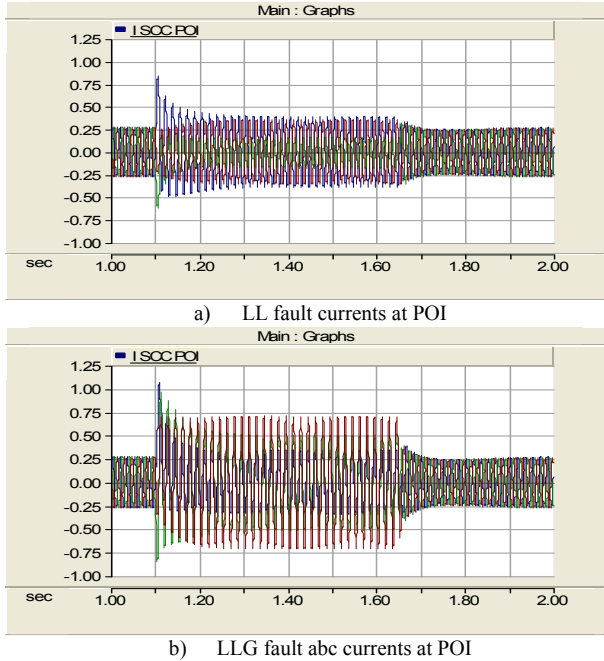


Figure 16: Phase currents at the POI for a) LL fault and b) LLG fault

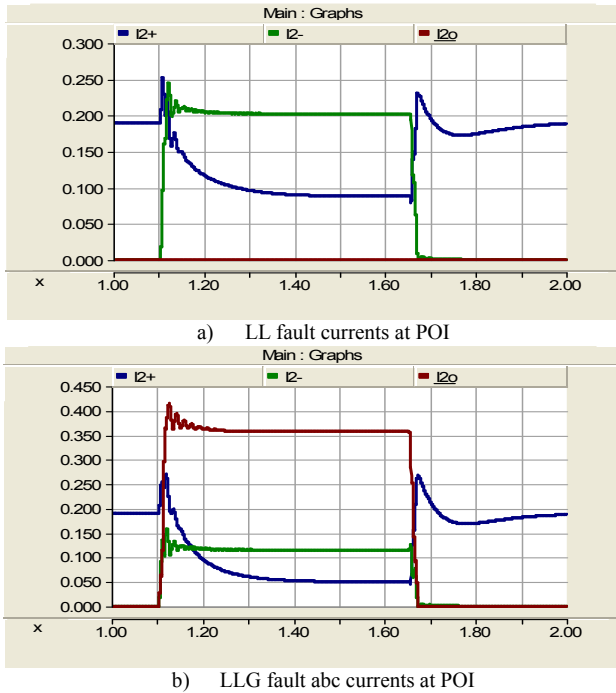


Figure 17: Sequence currents at the POI for a) LL fault and b) LLG fault

#### IV. CONCLUSIONS

In this paper, the SCC contributions of different WTGs for faults at the terminal of the generator were simulated using time domain simulations and steady-state calculations. Two power system commercial software platforms were used (PSCAD<sup>TM</sup>, and Cyme<sup>TM</sup>), and a multipurpose mathematical computer program (MathCAD<sup>TM</sup>) is also used to compute the SCC.

A simplified method to compute the SCC for a symmetrical fault is presented and it is tabulated in Table I. The SCC results were tabulated in Table II, comparing the size of the SCC at the POI for three different methods. Note that only Type 1 and Type 4 WTGs are used because they represent the maximum and minimum SCC contribution. The calculations for Type 2 and Type 3 WTGs are affected by time-of-fault occurrence and the action of the external rotor resistance control and the crowbar action, thus, the SCC contribution is usually lower than the Type 1 WTG, but it is higher than the Type 4 WTG.

The unsymmetrical faults were simulated and tabulated. As shown in the Table III through Table V, the unsymmetrical fault calculations from three different software packages shows a good agreement for unsymmetrical fault calculations.

Each WPP is unique. Therefore, recommended practice from local reliability organizations, manufacturers, transmission planners, wind plant developers, and local utilities should be followed very closely when performing studies of WPP.

#### V. ACKNOWLEDGMENT

This work is supported by the U.S. Department of Energy. The authors wish to acknowledge the technical support from Cyme and PSCAD during the development of this paper.

#### VI. REFERENCES

- [1] U.S. Department of Energy – Energy Efficiency and Renewable Energy, “20% Wind Energy by 2030 – Increasing Wind Energy’s Contribution to U.S. Electricity Supply,” May, 2008.
- [2] J. Charles Smith, Michael R. Milligan, Edgar A. DeMeo and Brian Parsons, “Utility wind Integration and operating impact state of the art,” *IEEE Trans. Power Systems*, vol. 22, pp. 900-908, Aug. 2007.
- [3] IEEE PES Wind Plant Collector System Design Working Group, “Wind Power Plant Grounding, Overvoltage Protection, and Insulation Coordination,” Proceedings of the 2009 IEEE Power and Energy Society General Meeting.
- [4] Nader Samaan, Robert Zavadil, J. Charles Smith and Jose Conto, “Modeling of Wind Power Plants for Short Circuit Analysis in the Transmission Network,” in *Proc. of IEEE/PES Transmission and Distribution Conference*, Chicago, USA, April 2008.
- [5] J. Moren, S.W.H. de Haan, “Short-Circuit Current of Wind Turbines with Doubly Fed Induction Generator,” *IEEE Transactions on Energy Conversion*, Vol. 22, No. 1, March 2007.
- [6] Sulawa, Zabara, et al. Short circuit current of induction generators. IEEE ISCAS 2007 proceedings.
- [7] E. Muljadi, V. Gevorgian, “Short Circuit Modeling of a Wind Power Plant,” in Proc. 2011 IEEE Power Engineering Society General Meeting.

## VII. BIOGRAPHIES



**Vahan Gevorgian** (M'97) graduated from the Yerevan Polytechnic Institute (Armenia) in 1986. During his studies he concentrated on electrical machines. His thesis research dealt with doubly-fed induction generators for stand-alone power systems. He obtained his Ph.D. degree in Electrical Engineering Dept. from the State Engineering University of Armenia in 1993. His dissertation was devoted to a modeling of electrical transients in large wind turbine generators.

Dr. Gevorgian is currently working at the National Wind Technology Center (NWTC) of National Renewable Energy Laboratory (NREL) in Golden, Colorado, USA, as a research engineer. His current interests include modeling and testing of various applications of small wind turbine based power systems.



**Mohit Singh** (M'2011) received his M.S. and Ph.D. in Electrical Engineering from the University of Texas, Austin in 2007 and 2011 respectively. His research is focused on dynamic modeling of wind turbine generators.

Dr. Singh is currently working at the National Renewable Energy Laboratory (NREL) in Golden, Colorado, USA, as a post-doctoral researcher in transmission and grid integration of renewable energy. His current interests include modeling and testing of various applications of wind turbine generators and other renewable energy resources. He is a member of the IEEE. He is involved in the activities of the IEEE Power and Energy Society (PES).



**Eduard Muljadi** (M'82-SM'94-F'10) received his Ph. D. (in Electrical Engineering) from the University of Wisconsin, Madison. From 1988 to 1992, he taught at California State University, Fresno, CA. In June 1992, he joined the National Renewable Energy Laboratory in Golden, Colorado. His current research interests are in the fields of electric machines, power electronics, and power systems in general with emphasis on renewable energy applications. He is member of Eta Kappa Nu, Sigma Xi and a Fellow of the IEEE. He is involved in the activities of the IEEE Industry Application Society (IAS), Power Electronics Society, and Power and Energy Society (PES).

He is currently a member of various committees of the IAS, and a member of Working Group on Renewable Technologies and Dynamic Performance Wind Generation Task Force of the PES. He holds two patents in power conversion for renewable energy.